Journal of Catalysis **189,** 195–208 (2000)
Article ID jcat.1999.2695, available online at http://www.idealibrary.com on IDEAL®

Effects of Oxidation–Reduction and Oxychlorination–Reduction Cycles on Pt–Ge/Al_2O_3 Catalysts

Geomar J. Arteaga, James A. Anderson, and Colin H. Rochester

Department of Chemistry, Dundee University, Dundee DD1 4HN, UK

Received July 8, 1999; revised September 10, 1999; accepted September 28, 1999

Two Pt(0.3%)–Ge/Al_2O_3 catalysts containing 0.15 and 0.45% Ge have been characterized by CO chemisorption and FTIR spectra of adsorbed CO after series of oxidation/reduction and oxychlorination/reduction cycles and have also been used for the catalytic hydroreforming of heptane. Catalysts after oxychlorination contained chloro- and oxychloro-Pt complexes which were responsible for the efficient spreading of Pt over the support surface and hence for the maintenance of a good Pt dispersion after reduction. XRD study of a more highly loaded catalyst gave no evidence for Pt–Ge alloy formation or for Ge^0 species. Reduced Cl-containing catalysts contained small clustered arrays of Pt atoms dispersed possibly as mats rather than particles over the GeO_x-modified alumina such that all the exposed Pt atoms were influenced by an electron withdrawing effect of both Ge^{2+} ions and Cl ions. Germanium did not block low-coordination Pt sites but may have partially decorated arrays of high coordination sites. Germanium partially stabilized Pt/Al_2O_3 against loss of activity through coking. The dominant mutual effect of Ge and Cl in catalysts was a significant loss in hydrogenolysis selectivity, but gains in the selectivities of aromatization, isomerization, and cyclization reactions. The addition of Ge to Pt/Al_2O_3 did not compromise the availability of Pt adsorption sites and only reduced by a small amount the turnover frequencies for heptane reforming reactions. Good activities were therefore maintained in the absence of Ge^0 or alloy formation during catalyst reduction.

Key Words: **Pt–Ge/Al_2O_3, CO adsorption on; Pt–Ge/Al_2O_3, heptane reforming over.**

INTRODUCTION

The use of Pt–Ge/Al_2O_3 as a reforming catalyst at low pressure requires regular catalyst regeneration after sintering and coking and therefore the behavior of Pt–Ge/Al_2O_3 after oxidation/reduction and oxychlorination/reduction treatments is of the utmost importance, but has received scant attention. The present study attempts to remedy this deficiency by studying the effects of repeated oxidation/reduction cycles in the absence of Cl (1, 2) and oxychlorination/reduction cycles (3) on catalytic behavior (as monitored by heptane reforming reactions) and surface properties (CO chemisorption, FTIR of adsorbed CO). A catalyst containing high Pt and Ge loadings was studied by XRD in order to assess the effects of treatment conditions on bulk catalyst structures.

The reduction in hydrogen of Pt^{4+} to Pt^0 in Pt–Ge/Al_2O_3 catalysts is complete below 673 K, but the oxidation state of the Ge species after reduction depends on the method of catalyst preparation, metal loadings, and reduction conditions (4–7). Bouwman and Biloen (8) showed that Ge^{4+} and Ge^{2+} were present after reduction at 823 K, but after reduction at 923 K the catalyst contained Ge^{2+} with some Ge^0 probably alloyed with Pt. Alloy phases Pt_2Ge, PtGe, and Pt_2Ge_3 have been identified (9, 10). However, Goldwasser *et al.* (5) found no evidence for Ge^0 in a catalyst which had been reduced at temperatures up to 973 K, although Ge^0 in alloy and free Ge particles have been reported after reduction at 1073 K (4, 7). Bimetallic Pt–Ge, Pt_3Ge_2, and Pt_3Ge clusters have been reported for catalysts reduced at 673 K, although their formation was a function of catalyst preparation (6).

Alloying of Pt and Ge in Pt–Ge/Al_2O_3 catalysts can lead to significant losses in both dehydrogenation and hydrogenolysis activity (7). Activities for benzene hydrogenation and butane hydrogenolysis were decreased by increasing Ge loading, this being attributed to an electronic effect of Ge on Pt (5). However, for heptane reforming isomerization activity was also decreased by increasing Ge, but, in contrast, hydrogenolysis activity was increased (11). The activities of both reactions were enhanced by the addition of HCl during catalyst preparation (11), possibly because Cl partially inhibits alloy formation (4, 7). Catalytic behavior for octane reforming reactions was also dependent on the method of catalyst preparation (6). Coq *et al.* (12) have suggested from study of 2,2,3, 3-tetramethylbutane over Pt–Ge/Al_2O_3 that the addition of Ge marginally favored a shift to central cleavage, indicating that the properties of the surface Pt atoms were slightly shifted toward those characteristic of larger Pt particles.

EXPERIMENTAL

Chlorine-free Pt/Al_2O_3 catalyst precursors, designed to contain 0.3 and 3.0 wt% Pt after reduction, were prepared

0021-9517/00 $35.00

from tetraammine–platinum(II) hydroxide and γ-alumina (surface area 110 $m^2\ g^{-1}$) as before (13, 14), the final stage involving heating in air at 673 K. Subsequent impregnation with tetraethylgermane dissolved in heptane and solvent removal by evaporation at 318 K was followed by drying in air for 15 h at 383 K and then calcination for 1 h in dry CO_2-free air at 673 K. The compositions of the resulting three Pt–Ge/Al_2O_3 catalyst precursors were such as to give Pt(0.3 wt%)–Ge(0.15 wt%), Pt(0.30 wt%)–Ge(0.45 wt%), and Pt(3.0 wt%)–Ge(1.5 wt%) after reduction in hydrogen. These loadings are equivalent to Pt : Ge molar ratios of 1 : 1.34, 1 : 4.03, and 1 : 1.34, respectively.

Transmission infrared spectra of pressed discs of catalyst (20 mg cm^{-2}) at ca. 293 K were recorded at 4 cm^{-1} resolution with a Perkin Elmer 1710 FTIR spectrometer. Pulsed chemisorption of CO on catalyst powder at ca. 293 K was measured using a Perkin Elmer AutoSystem XL gas chromatograph. Powder XRD patterns were recorded using CuK_α radiation at 1° 2θ min^{-1}. A Perkin Elmer 8410 gas chromatograph with an FID and a 5.6-m column containing 15% squalane on chromosorb W-HP (80–100 mesh) was used to analyze the products of hydrogen/heptane reactions over 50 mg powdered catalyst under the conditions: 623 K; 1 atm pressure; 25 $cm^3\ min^{-1}$ hydrogen flow; (H_2/heptane) molar ratio (10/1); LHSV 18.2 cm^3 heptane (g cat)$^{-1}$ h^{-1}, <10% conversion.

Pt–Ge/Al_2O_3 catalyst precursors were initially subjected to a "calc" cycle which involved heating at 15 K min^{-1} to 673 K and holding at 673 K for 30 min in a flow of air followed by reduction for 1 h in flowing hydrogen. Reduced catalyst was then subjected in various sequences to two additional treatment cycles: (a) (designated "ox") oxidation in dry CO_2-free air for 1 h at 823 K followed by reduction for 1 h in a hydrogen flow at 673 K, (b) (designated "oxy") oxychlorination for 1 h at 823 K in an air flow containing 31 μmol h^{-1} 1,2-dichloropropane per 50 mg of catalyst followed by reduction in a hydrogen flow for 1 h at 673 K. XRD, CO chemisorption, FTIR, or catalytic activity studies were carried out at various stages of the total treatment sequence for each catalyst.

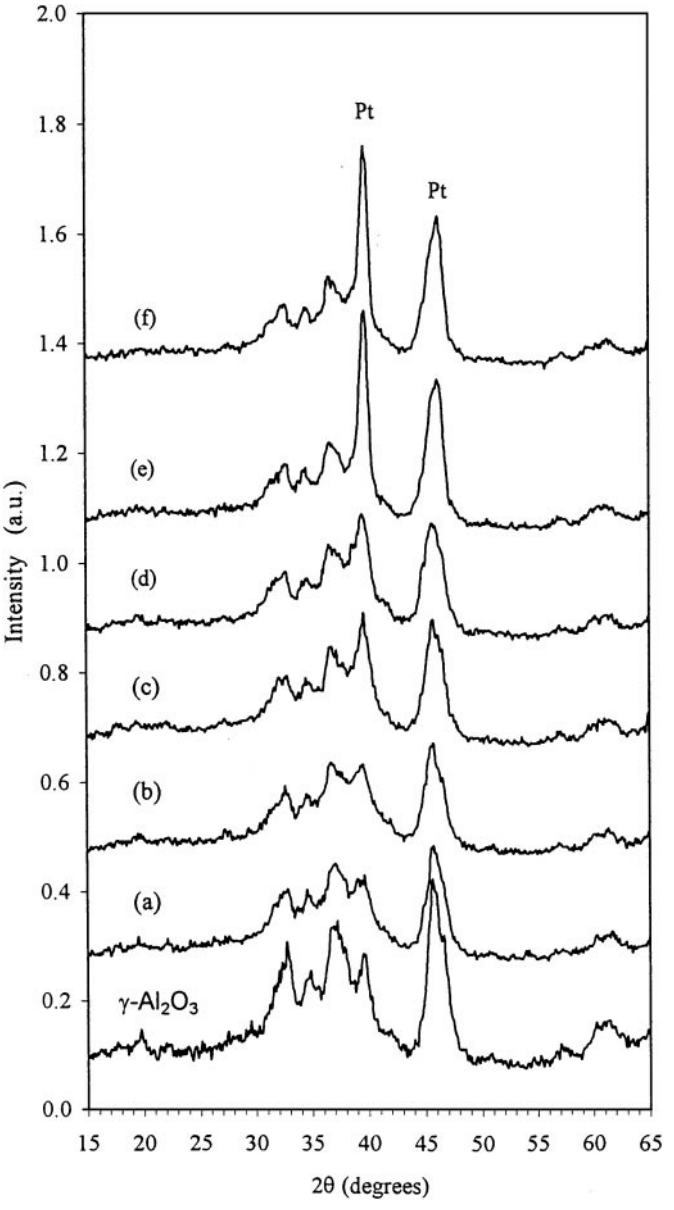

FIG. 1. XRD patterns for alumina alone and after the Pt(3%)–Ge(1.5%)/Al_2O_3 catalyst precursor was subjected to (a) calcination, (b) a calc cycle, (c) a calc cycle and oxidation, (d) a calc cycle and an ox cycle, (e) a calc cycle and oxychlorination, and (f) a calc cycle and an oxy cycle.

RESULTS

XRD Results

The catalysts containing 0.3% Pt and 0.15 or 0.45% Ge gave no detectable peaks due to Pt or Ge species after all the treatments adopted here. Figure 1 shows XRD results for the more highly loaded Pt(3%)–Ge(1.5%)/Al_2O_3 catalyst. The pattern for catalyst calcined in air at 673 K closely resembled that for alumina alone. There was no evidence for PtO_2 or GeO_2, which, if they existed in the catalyst, were, well-dispersed. Subsequent reduction gave a slight enhancement at $2\theta = 39.8°$, where a peak due to Pt^0 coincides with one of the peaks due to alumina. The peak due to Pt^0 was enhanced by oxidation at 823 K showing that decomposition of PtO_2 to Pt^0 had occurred. Reduction after oxidation had negligible additional effect, suggesting that little reducible PtO_2 remained at the end of the oxidation treatment. After oxychlorination the Pt^0 peak became narrower and more intense, suggesting not only that the Pt was well reduced, but also that bigger crystallites of Pt^0 were formed than after oxidation in the absence of chlorine. The difference was maintained after subsequent reduction. There was no evidence in any of the XRD patterns for GeO_2, suggesting that oxidic Ge was well dispersed over

the alumina surface, or for the possible bimetallic alloys (3, 6) Pt_3Ge, Pt_3Ge_2, PtGe, Pt_2Ge_3, and $PtGe_2$.

Infrared Spectra of Adsorbed CO

The spectroscopic results for Pt(0.3%)–Ge(0.15%)/Al_2O_3 and Pt(0.3%)–Ge(0.45%)/Al_2O_3 were similar and therefore only spectra for the latter are given in Fig. 2, where the CO pressure was the highest studied and gave complete coverage of all the available Pt sites. Spectra contained a band at ca. 2202 cm^{-1} due to weakly adsorbed CO on Al^{3+} sites on alumina. After calc or ox cycles a dominant band at 2071 cm^{-1} and a shoulder at 2080 cm^{-1} are ascribable to linearly adsorbed CO on Pt (15). At low coverages with 0.04 Pa CO the envelope maximum was at ca. 2064 cm^{-1}, the shift to higher wavenumber with increasing

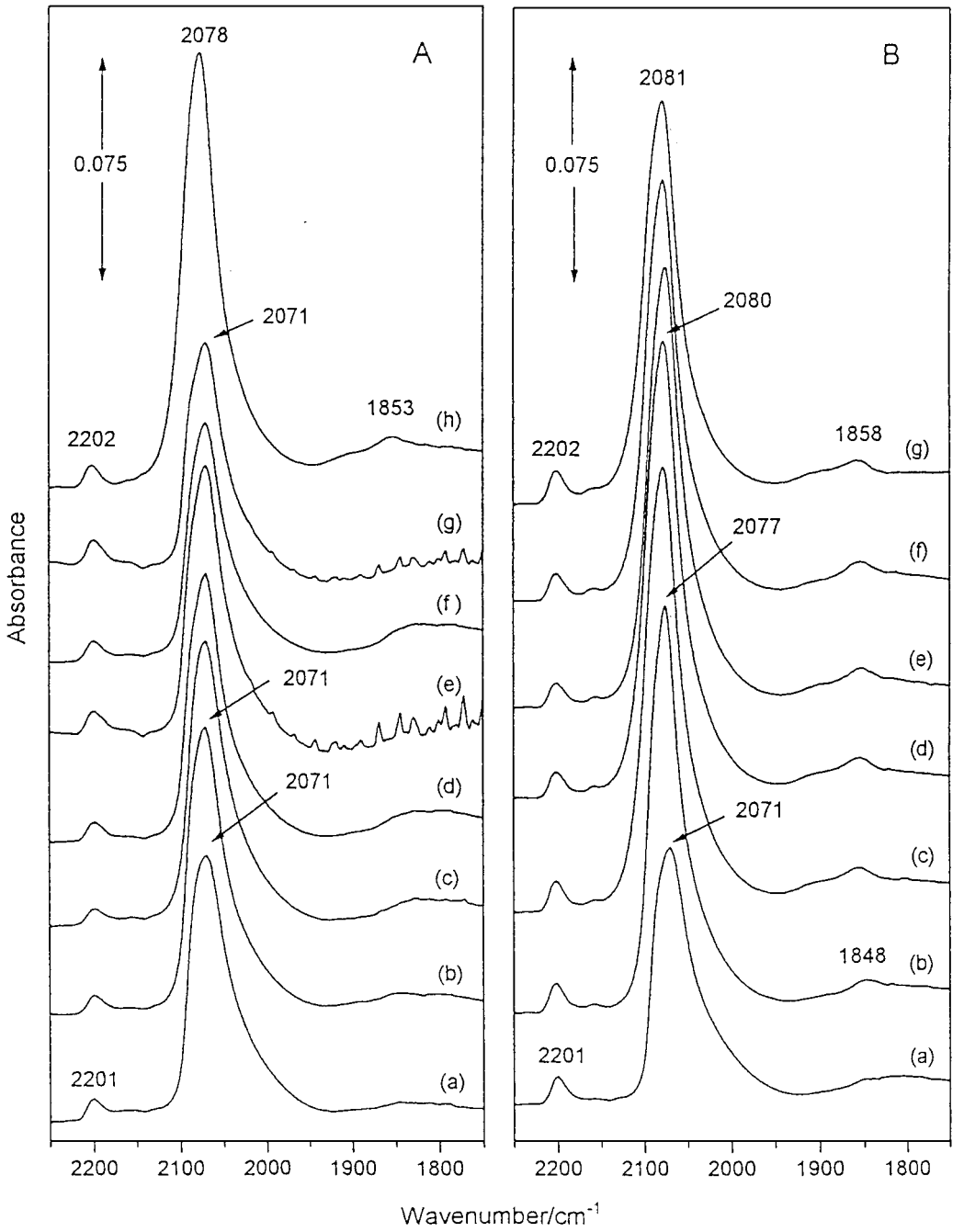

FIG. 2. Spectra of CO (6.7 kPa) adsorbed on Pt(0.3%)–Ge(0.45%)/Al_2O_3 after (a) a calc cycle, and (A) (b)–(g) each of six consecutive ox cycles and (h) finally an oxy cycle and (B) (b)–(g) six consecutive oxy cycles.

coverage being attributable to either increasing dipolar coupling effects between adjacent adsorbed CO molecules (15) or the presence of a smaller number of surface Pt atoms of lower coordination (constituting stronger adsorption sites) than the majority of the exposed Pt atoms (14, 16). For $Pt(0.3\%)/Al_2O_3$ after ox cycles the maximum was at 2072 cm^{-1} for high CO coverages, similar to the band position here, but was at ca. 2039 cm^{-1} for low coverages, much lower than here (14). The assignment of the latter band to step or edge sites suggests that its absence in the presence of germania was due to either blocking of these intermediate coordination sites (16) by germanium or decreased electron density at the sites. The latter could result from electron transfer from Pt to oxidic germania spread on the alumina surface. Compared with Pt/Al_2O_3 (14), $Pt–Ge/Al_2O_3$ also gave a weaker maximum at ca. 1850 cm^{-1} due to bridging CO (15).

The areas under the maxima due to linearly adsorbed CO decreased with each successive ox cycle to which catalysts were subjected in accordance with the expected effects of catalyst sintering in the absence of chlorine (1, 3). In Fig. 3 band areas are normalized for each disc by division by the area for the disc after a calc cycle. The band areas were significantly increased by oxy cycles no matter whether they were preceded by calc or ox cycles. This parallels a corresponding effect of oxychlorination for Pt/Al_2O_3, and may be attributed to favorable spreading of Pt-oxychloro complexes over alumina during oxychlorination, which in turn favors an enhanced Pt dispersion after reduction (3). The variations of CO/Pt from chemisorption measurements (Fig. 3) confirm the implications of the infrared intensity data. The CO/Pt values also show that the Pt dispersions for the two Ge loadings were closely similar to each other. Pt–Ge catalysts after calc or ox cycles were less well dispersed than Pt alone (e.g., dispersion after a calc cycle from ca. 0.5 for Pt to ca. 0.4 for Pt–Ge), whereas after oxy cycles the Pt dispersions for Pt–Ge were slightly better than those for Pt alone (14).

The maximum for linear CO was shifted by about 9 cm^{-1} to higher wavenumbers after oxy cycles as opposed to calc or ox cycles, and there was no obvious higher wavenumber shoulder on the band envelope. The band shift suggests that Pt was in an enhanced electron-deficient state as previously concluded (8) for the effect of Ge on a Cl-containing $Pt–Al_2O_3$ catalyst. Electron withdrawal from Pt could have involved an interaction with oxidic germania species distributed over the alumina surface. Residual Cl-adatoms on the catalyst surfaces may also have provided an e-withdrawing effect on platinum.

Adsorption of CO after oxy cycles gave a stronger band at ca. 1850 cm^{-1} due to bridging CO than for Cl-free catalyst, the band being weaker with 0.45% Ge loading than with 0.15% Ge. Enhanced dispersion of Pt promoted by the presence of chlorine was accompanied by an increase in the

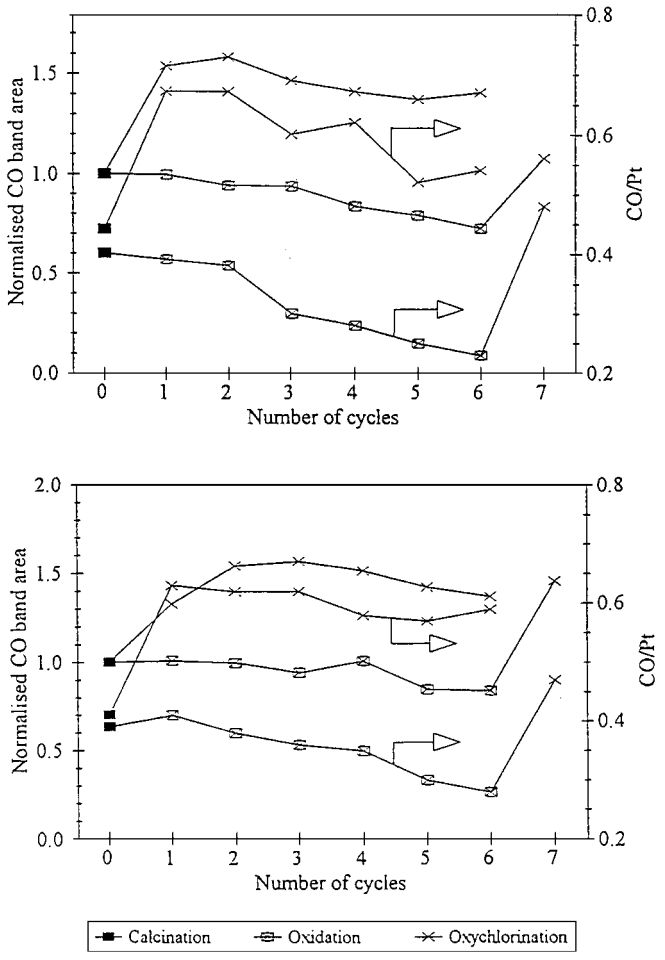

FIG. 3. Normalized CO infrared band areas and CO/Pt chemisorption results for reduced $Pt(0.3\%)–Ge(0.15\%)/Al_2O_3$ (top) and $Pt(0.3\%)–Ge(0.45\%)/Al_2O_3$ (bottom) as a function of treatment cycles.

proportion of bridging sites which with CO gave an infrared band at the same position as that for Pt alone (14). This contrasts with the effect of added Sn on Pt/Al_2O_3, where for Cl-containing catalyst the band at ca. 1850 cm^{-1} was replaced by a band at ca. 1900 cm^{-1} (14). The latter band also appeared in the spectra for $Pt–Ge/Al_2O_3$ and has been attributed to a Cl_2Pt_2CO complex adjacent to a modified alumina surface (14).

Spectra of CO adsorbed on oxychlorinated $Pt–Ge/Al_2O_3$ catalysts (Fig. 4) have been recorded before reduction. Band assignments have been discussed before in relation to corresponding studies of Pt/Al_2O_3 and $Pt–Sn/Al_2O_3$ (14).

For catalyst with 0.15% Ge (Fig. 4A), the band at 2093 cm^{-1} appearing at low CO pressure was due to linear CO on Pt^0 surfaces covered with O-adatoms (15). Bands at 2141 and 2158 cm^{-1}, which grew with increasing CO pressure, are attributed to Cl complexes of Pt containing ligated CO (3, 14). A shoulder at ca. 2118 cm^{-1} resembles a band for CO on PtO_2 (17). At the highest CO pressures bands appearing at 2132 and 2171 cm^{-1}, which remained after

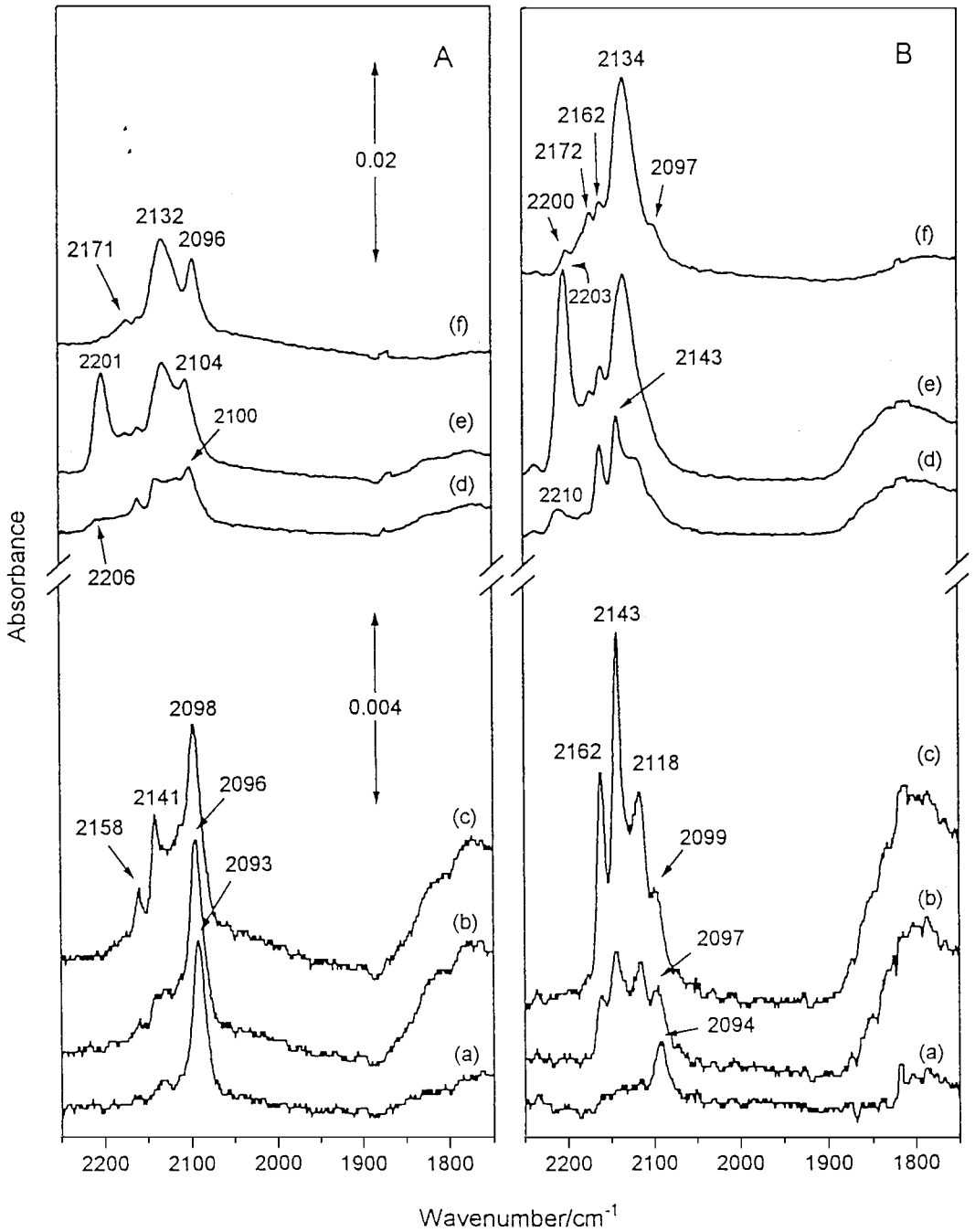

FIG. 4. Spectra of (A) Pt(0.3%)–Ge(0.15%)/Al_2O_3 after an oxy cycle following one calc and six ox cycles and (B) Pt(0.3%)–Ge(0.45%)/Al_2O_3 after an oxy cycle following a calc cycle, exposed to CO at (a) 0.05, (b) 0.11, (c) 0.53, (d) 133, and (e) 6670 N m^{-2} (with gas-phase bands subtracted) and (f) after subsequent evacuation.

evacuation, may be ascribed to CO ligated to oxychloro-Pt species spread over the Al_2O_3 support (13, 14). Overall the pattern of behavior for CO interacting with Pt-containing species in Pt(0.3%)–(0.15%)/Al_2O_3 closely resembled corresponding results for Pt(0.3%)–Sn(0.3%)/Al_2O_3 (14). However, a band at 1750–1800 cm^{-1}, due to adsorption on the alumina support (18, 19) remained as prominent for Pt–Ge catalysts as for Pt alone, whereas it was very weak for Pt–Sn catalysts (14). One explanation would be that Ge species were not as extensively spread as Sn species over the alumina surface and therefore blocked fewer of the alumina sites which adsorbed CO. However, an alternative explanation would be that Ge species and Sn species were spread to the same extents but the Ge species

provided similar sites for CO adsorption as those provided by unmodified alumina.

The results for CO adsorption on Pt(0.3%)–Ge(0.45%)/Al_2O_3 after oxychlorination (Fig. 4B) were nearly identical to those for Pt/Al_2O_3 in the absence of Ge (14). For Pt(0.3%)–Ge(0.45%)/Al_2O_3 residual bands at 2162 and 2200 cm^{-1} after evacuation resembled bands for $Cl_2Pt(CO)_2$ (20).

Heptane Reforming Reactions

Catalyst activities and selectivities were measured after 5 min ("initial" values) and up to 8 h ("final" values) on line. Activities decreased with time in the early stages of reaction but remained fairly steady after ca. $2\frac{1}{2}$ h. Initial and final activities as a function of series of treatment cycles are shown in Fig. 5. The addition of 0.15% Ge reduced the initial activity after a calc cycle to about 36% of its value for Pt(0.3%)/Al_2O_3 (21). However, the addition of 0.45% Ge partially reversed this change giving an initial activity which was 56% of the activity for Pt alone. Combination of the initial activities with the measured CO/Pt values for catalysts after a calc cycle gave estimated turnover frequencies (TOFs) of 0.46, 0.22, and 0.38 s^{-1} for catalysts containing 0, 0.15, and 0.45% Ge, respectively. TOFs after the first ox cycle for each catalyst were 0.38, 0.18, and 0.23 s^{-1}. Decreases in activity with time were slightly less for Pt–Ge catalysts than for Pt alone, suggesting that Ge partially inhibited coking of active sites (14, 16). As for Pt/Al_2O_3 (1, 14), repeated ox cycles for Cl-free Pt–Ge/Al_2O_3 catalysts progressively reduced catalytic activity (Fig. 3), although the effect was smaller in the presence of Ge. This parallels a smaller decrease in CO/Pt for Pt–Ge than for Pt alone with increasing number of ox cycles showing that losses of surface area due to progressive catalyst sintering (1, 3, 14) were partially inhibited by the addition of Ge to Pt/Al_2O_3.

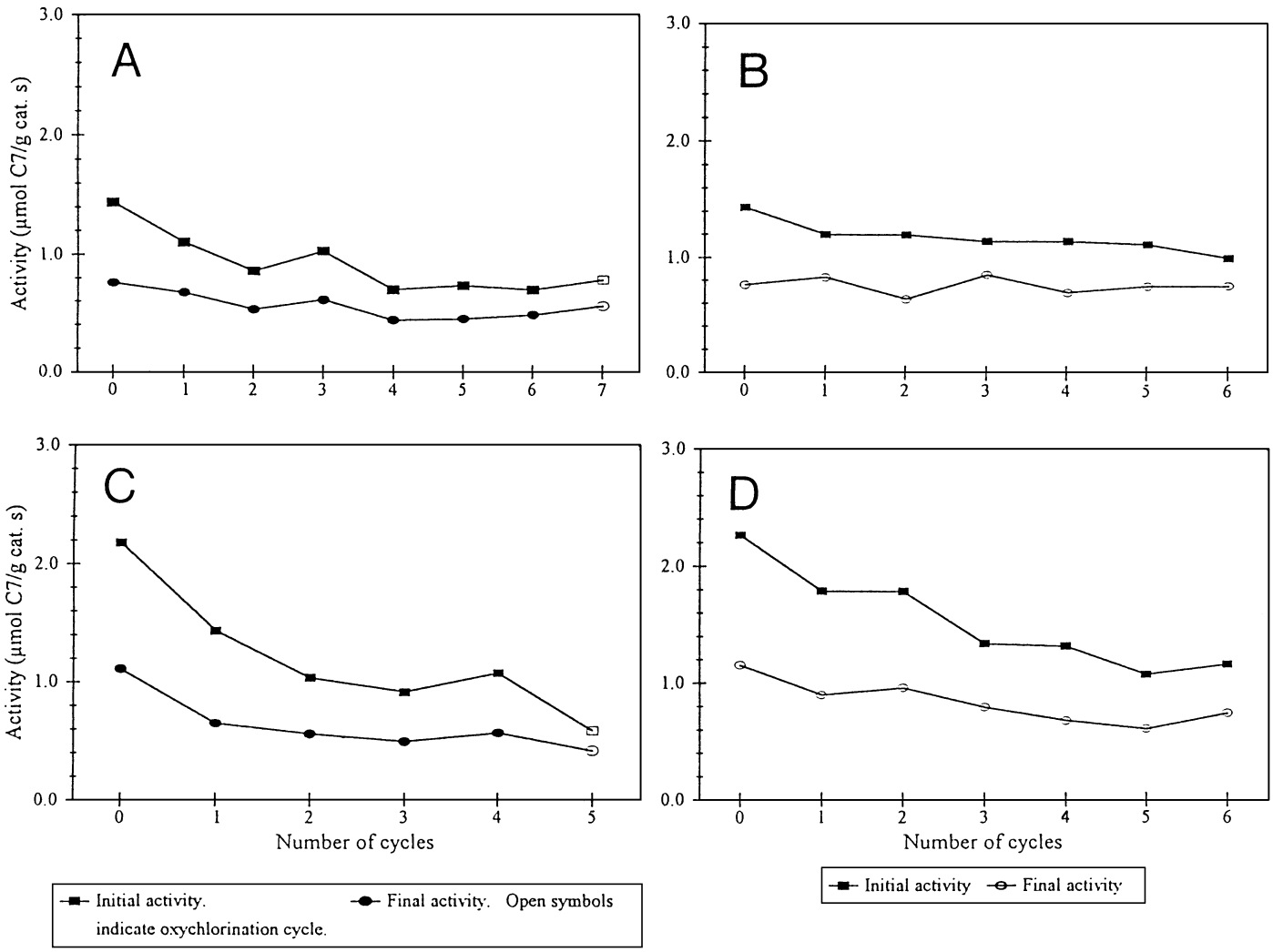

FIG. 5. Heptane reforming activities over (A), (B) Pt(0.3%)–Ge(0.15%)/Al_2O_3, and (C and D) Pt(0.3%)–Ge(0.45%)/Al_2O_3 after series of cycles starting with calc (cycle 0) and followed by (A) six or (C) four ox cycles followed by an oxy cycle or (B and D) six oxy cycles.

For Pt alone repeated oxy cycles maintained high activity (2, 21). However, the beneficial effect of chlorine, although being maintained to some extent for Pt–Ge/Al_2O_3, was less significant. Losses in activity with increasing number of oxy cycles occurred, particularly for Pt–Ge(0.45%)/Al_2O_3. Activity loss also occurred for the first oxy cycle after the initial calc cycle despite the fact that the first oxychlorination generated a much improved Pt dispersion (Fig. 3). Thus the TOF per exposed Pt atom was reduced by oxychlorination, the TOFs following a first oxy cycle being 0.38, 0.12, and 0.19 s^{-1} for Ge loadings of 0, 0.15, and 0.45%, respectively. This is further borne out by the effects of an oxy cycle following several ox cycles when a small increase in activity (Fig. 5A) or a decrease in activity (Fig. 5C) were both paralleled by a large improvement in Pt dispersion (Fig. 3). The TOF for 0.45% Ge loading fell to 0.13 s^{-1} after the fifth consecutive oxy cycle.

The 21 observed reaction products have been grouped according to whether they were formed by aromatization (toluene was dominant with less than 0.5% of the total aromatization giving benzene), cyclization (to saturated cyclics), isomerization, or hydrogenolysis reactions. In general for Cl-free catalysts after calc and ox cycles the selectivities for Pt(0.3%)–Ge(0.15%)/Al_2O_3 (Fig. 6) compared with those for Pt(0.3%)/Al_2O_3 (21) showed that the addition of Ge decreased aromatization and hydrogenolysis, but increased cyclization and isomerization. Increasing the Ge content to 0.45% had little further effect other than, if anything, slightly reducing cyclization and slightly increasing hydrogenolysis.

The C_1/C_3 ratios for hydrogenolysis over Cl-free Pt(0.3%)–Ge(0.15%)/Al_2O_3 (Fig. 7) were slightly greater than the corresponding ratios for Pt/Al_2O_3 (21). However, ratios (Fig. 7) of the isomerization products 2-methylhexane (2MH), 3-methylhexane (3MH), and 3-ethylpentane (3EP) were more strongly influenced by Ge addition, which, in general after calc or ox cycles, decreased 2MH/3MH, increased 3EP/2MH, and left 3EP/3MH about the same. The overall increase in isomerization selectivity is therefore reflected in preferential increases in 3EP and 3MH rather than 2MH. The results for Cl-free Pt(0.3%)–Ge(0.45%)/Al_2O_3 showed more variations in selectivity ratios as a function

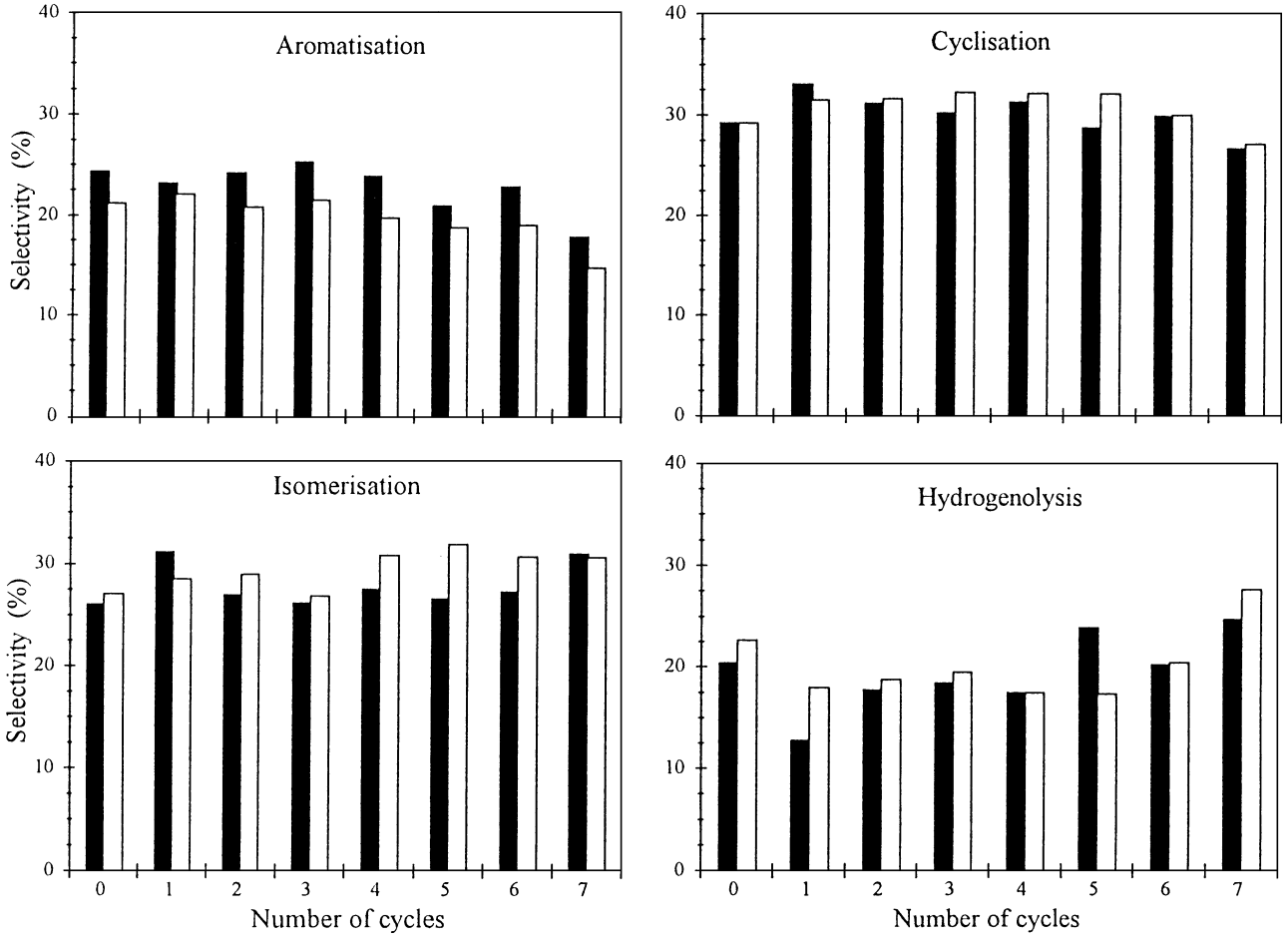

FIG. 6. Initial (shaded columns) and final (open columns) selectivities for Pt(0.3%)–Ge(0.15%)/Al_2O_3 after a consecutive series of cycles involving a calc (cycle 0), six ox (cycles 1–6), and an oxy (cycle 7) treatments.

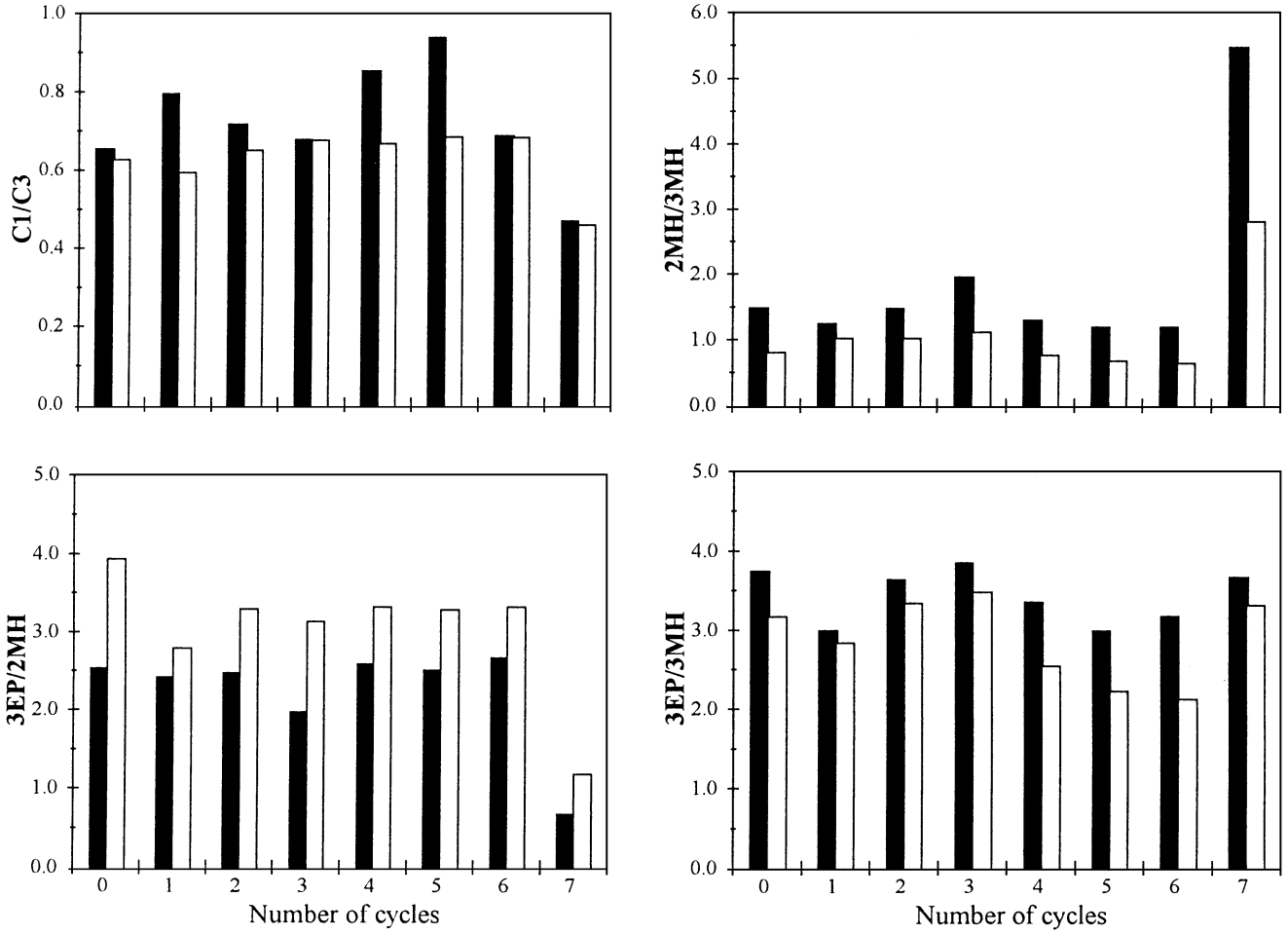

FIG. 7. Ratios of hydrogenolysis and isomerization products for the same conditions as in Fig. 6.

of cycle number. However, in general C_1/C_3 and 3EP/3MH values were less, 2MH/3MH was slightly less, and 3EP/2MH was about the same for the higher Ge loading.

The dominant cyclic products were 1,2-dimethylcyclopentane (DMCP) and ethylcyclopentane (ECP) with never more than 1.2% of the total cyclized products being methylcyclohexane. Ratios of DMCP/ECP for catalysts containing 0, 0.15, and 0.45% Ge after one ox cycle were 0.20, 0.27, and 0.20, respectively. After a fifth consecutive ox cycle the corresponding ratios were 0.17, 0.30, and 0.19.

Reaction selectivities were remarkably stable during sequences of oxy cycles (Fig. 8). The presence of 0.15% Ge in Cl-containing Pt/Al_2O_3 considerably decreased hydrogenolysis selectivity from, on average, about 45 to 22% but increased isomerization selectivity from 18 to 28%, cyclization selectivity from 19 to 28%, and aromatization selectivity from 18 to 22%. The comparisons between Cl-free Pt/Al_2O_3 and Cl-free $Pt–Ge/Al_2O_3$ or between Cl-free $Pt–Ge/Al_2O_3$ and Cl-containing $Pt–Ge/Al_2O_3$ showed smaller changes, partially because the effects of adding Cl to Pt/Al_2O_3 were to increase hydrogenolysis and decrease isomerization, cyclization, and aromatization (21) in opposition to the corresponding effects of adding Ge. The effects of adding chlorine were less for Pt–Ge catalysts than for Pt alone. The big selectivity changes resulting from the addition of 0.15% Ge to Cl-containing catalyst was not further enhanced by increasing the Ge loading to 0.45%.

C_1/C_3 ratios were similar at ca. 0.55 for oxychlorinated Pt and Pt–Ge catalysts independent of Ge content. However, the addition of 0.15% Ge increased 2MH/3MH (from 2.9 to 3.7), decreased 3EP/2MH (from 1.6 to 0.9), and decreased 3EP/3MH (from 4.7 to 3.5). Increasing the Ge-content to 0.45% further enhanced the changes in 2MH/3MH and 3EP/2MH, giving average ratios of 7.0 and 0.6, respectively, but gave ca. 5 for 3EP/3MH which represents a reversal in behavior. Comparison of the data for Cl-free (Fig. 7) and Cl-containing $Pt(0.3\%)–Ge(0.45\%)/Al_2O_3$ (Fig. 9) shows that whereas oxychlorination had little effect on the C_1/C_3 and 3EP/3MH ratios, there was a big increase in 2MH/3MH and a big decrease in 3EP/2MH because 2MH had become a more significant product. Also, for both Cl-free (Fig. 7) and Cl-containing (Fig. 9) $Pt–Ge/Al_2O_3$, as for Pt/Al_2O_3 (21),

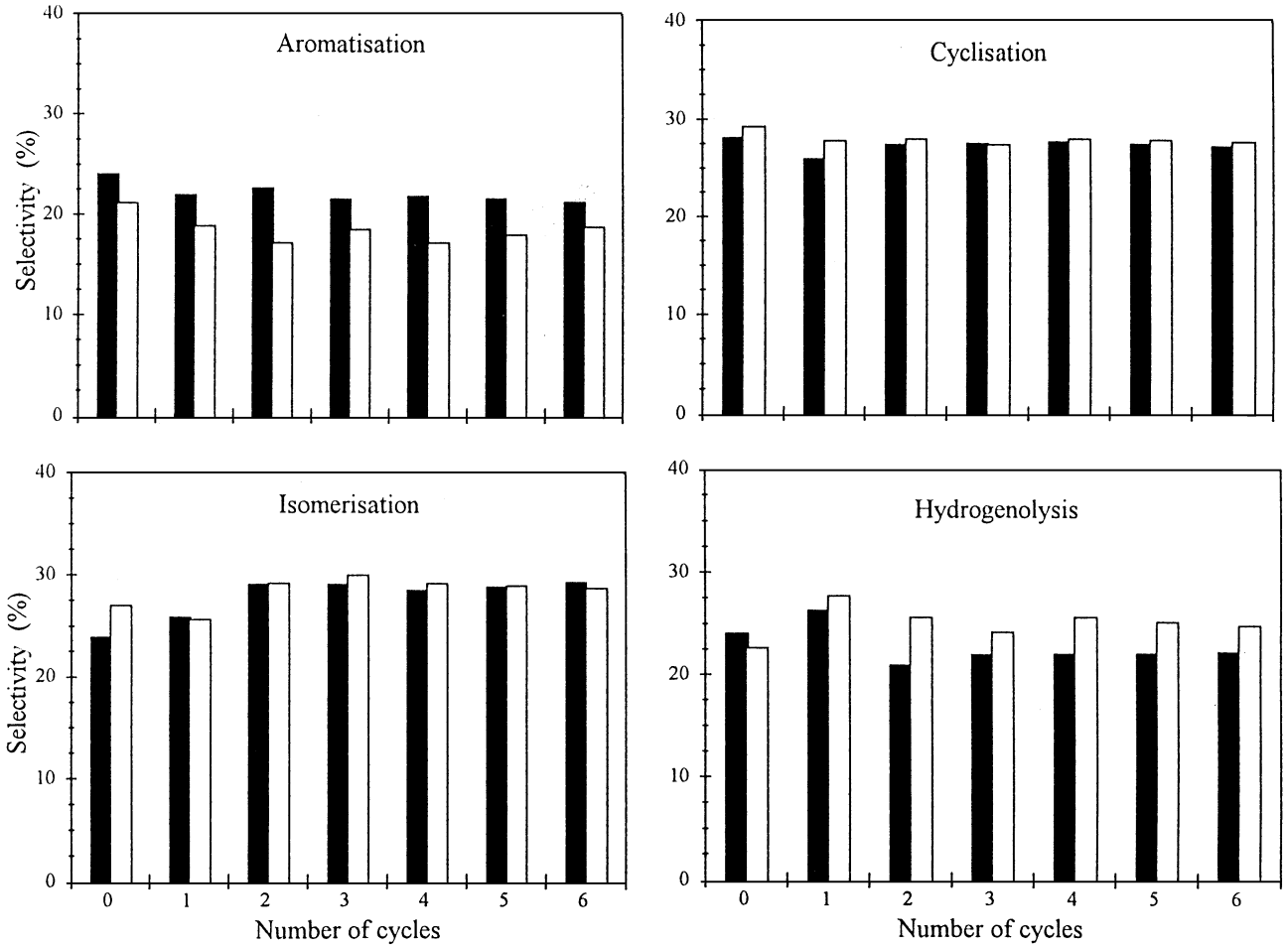

FIG. 8. Initial and final selectivities for Pt(0.3%)–Ge(0.15%)/Al_2O_3 after a consecutive series of cycles involving a calc (cycle 0) and six oxy cycles.

the 2MH/3MH and 3EP/2MH ratios were changed downward and upward, respectively, with increasing reaction time. catalyst deactivation by coking (16) reduced 2MH formation relative to the other two cyclic products.

Ratios DMCP/ECP for the formation of cyclization products over Cl-containing catalysts were insensitive (values in the range 0.19–0.22 with no obvious trends) to the addition of either 0.15 or 0.45% Ge. The only exception was for Pt(0.3%)–Ge(0.15%)/Al_2O_3 which gave a ratio of 0.29 after the first oxy cycle following six ox cycles. This value resembles that (0.30) after the final ox cycle, suggesting, as was observed for Pt–Sn/Al_2O_3 (14), that ox cycles generated catalyst structures which could not wholly be converted to the equilibrium structures resulting from oxy cycles in a single oxy cycle.

DISCUSSION

The States of Pt and Ge, and Pt Dispersion

The absence of XRD evidence for bulk phase Pt^0–Ge^0 alloys (6, 9, 10) after an ox or oxy cycle for the high-loaded catalyst contrasts with the result for Pt–Sn/Al_2O_3 catalyst for which the presence of chlorine induced the formation of bulk Pt^0–Sn^0 alloy of 1:1 stoicheiometry (13). The present result is consistent with observations that the germanium in Pt–Ge/Al_2O_3 catalysts which have been reduced at 673 K (6), 823 K (8), or even as high as 973 K (5) is predominantly in the Ge^{4+} and Ge^{2+} states. However, other studies showed that some Ge^0 may be present after reduction at 673 K (6), 773 K (3, 7, 22–24), or 923 K (8). The extent of reduction of Ge apparently depends not only on reduction temperature, but also reduction time (7) and the method of catalyst preparation (6). In accordance with the result here, Huang *et al.* (6) found that Pt(0.3%)–Ge(0.3%)/Al_2O_3 prepared by the successive impregnation of alumina with Pt and then Ge contained no Ge^0 after reduction at 673 K. The loading of Pt in their catalyst was identical to that in the low-loaded catalysts here, and the Ge loading was intermediate between the present loadings. We therefore conclude that low-loaded catalyst here contained no Pt^0–Ge^0 alloy. The infrared spectra of adsorbed CO support this conclusion. The absence of XRD evidence for GeO_2 for catalysts after oxidation, oxychlorination, or reduction (Fig. 1) suggests, in

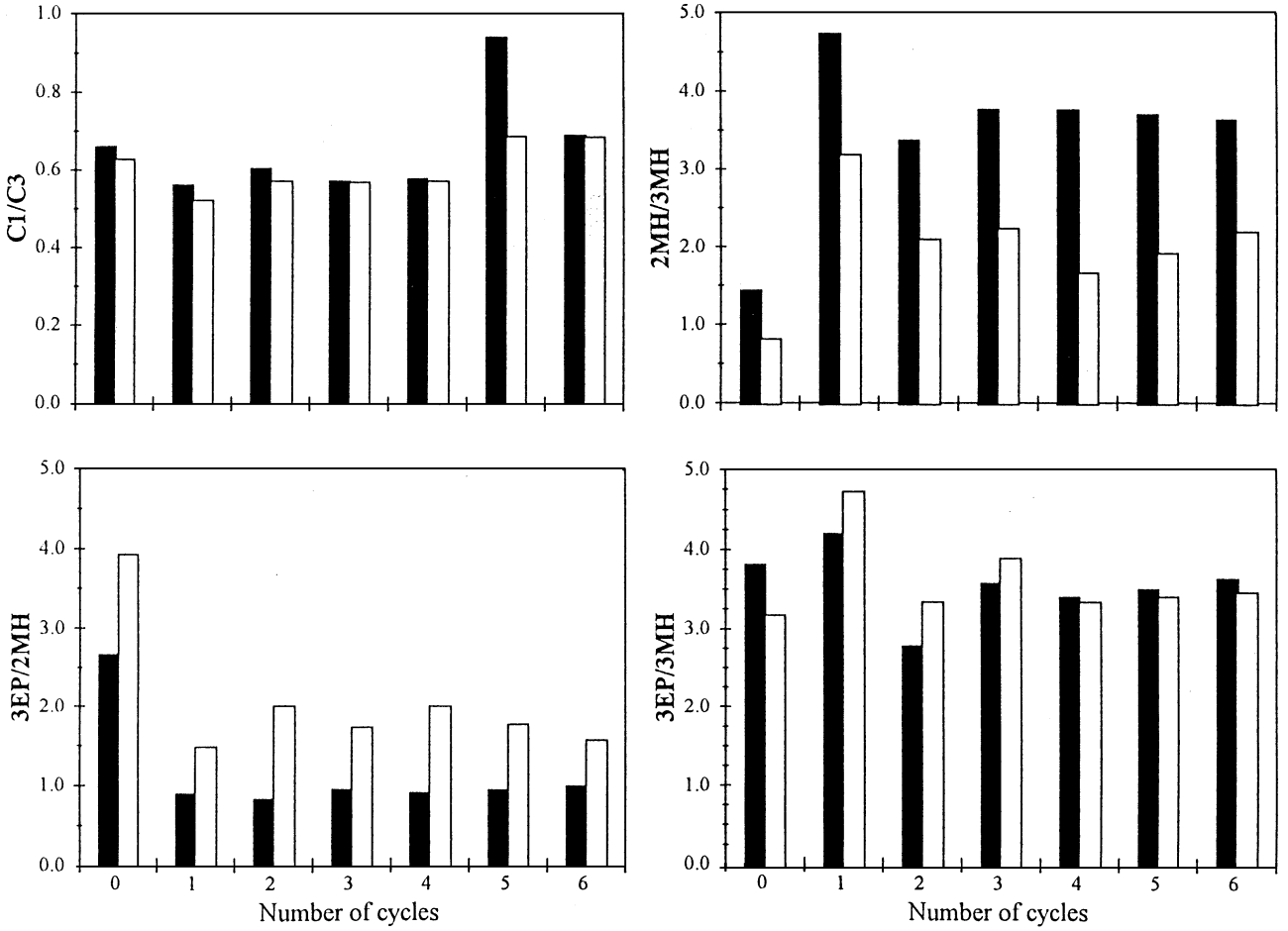

FIG. 9. Ratios of hydrogenolysis and isomerization products for the same conditions as in Fig. 8.

accordance with a conclusion from TEM work (6), that the oxidic Ge^{2+} and Ge^{4+} species (3, 7, 8) were closely bonded to and hence well spread over the alumina surface. The combined XRD and infrared results show that the Pt was present as Pt^0 particles with all exposed Pt atoms behaving as Pt^0, although possibly slightly modified electronically by interaction with other species on either the Pt surface or an adjacent Ge-modified alumina support surface.

Previous results for Pt–Ge/Al_2O_3 catalysts which contained chlorine in their preparation (6, 7, 22–24) or were apparently Cl-free (24) showed that the addition of Ge to Pt/Al_2O_3 reduced the Pt dispersion in accordance with the present results for Cl-free Pt/Al_2O_3 (14) and Pt–Ge/Al_2O_3 catalysts. However, in contrast, were the slightly enhanced CO/Pt values for Cl-containing Pt–Ge/Al_2O_3 (Fig. 3) compared with Pt/Al_2O_3 (14). Goldwasser *et al.* (5) similarly found that the addition of Ge to Cl-containing Pt/Al_2O_3 could maintain or even increase the %Pt dispersion depending on preparation conditions. Bouwman and Biloen (8) also concluded that relatively more platinum is kept in exposed sites when Ge is added to Pt/Al_2O_3. The present result is directly linked to the beneficial effect (3) of Cl addition to Pt(0.3%)/Al_2O_3 catalysts in improving the Pt dispersion (14) also being applicable for Pt–Ge/Al_2O_3. In the presence of Cl after oxy cycles Ge did not compromise the availability of exposed Pt surface sites. This contrasts with the result for Pt–Sn/Al_2O_3 where Sn addition reduced Pt dispersion to a greater extent than Ge addition for Cl-free catalyst and obviated the beneficial effect of Cl addition on Pt dispersion (14).

In terms of improving %Pt dispersion the effect of Cl on Pt–Ge/Al_2O_3 catalysts resembled the corresponding effect on Pt/Al_2O_3, but not for Pt–Sn/Al_2O_3 (14). The quality of dispersion is related to the effectiveness with which chloro-Pt and oxychloro-Pt complexes are formed and spread over the support surface during oxychlorination prior to reduction (3, 14). Oxidic tin spread over alumina impairs the subsequent spreading of the Pt complexes, and therefore impairs the quality of dispersion after reduction (14). Unlike the result for Pt(0.3%)–Ge(0.45%)/Al_2O_3 (Fig. 4B), none of the Pt–Sn/Al_2O_3 catalysts previously studied (14) gave a spectrum of adsorbed CO after oxychlorination closely similar to the result for Pt/Al_2O_3. The spectra of Pt–Ge(0.45%)/Al_2O_3, as for

Pt/Al_2O_3 (14), exhibited strong bands due to both chloro- and oxychloro-Pt complexes and, furthermore, the two catalysts gave CO/Pt chemisorption values after reduction (Fig. 3) which were very close to each other (14). The Pt(0.3%)–Ge(0.15%)/Al_2O_3 catalyst pretreated with six ox cycles gave, after oxychlorination, weaker bands due to chloro- and oxychloro-Pt complexes, a stronger band due to CO on reduced Pt particles, and a lower Pt dispersion after reduction. After repeated ox cycles had led to Pt sintering, spreading of the chlorinated Pt complexes was less efficient during oxychlorination leading to an impaired Pt dispersion after subsequent reduction.

The Character of Pt Surface Sites

De Ménorval *et al.* (25) reported for Cl-free Pt–Ge/Al_2O_3 that the main ν(CO) band due to adsorbed CO at high coverage was at 2063 cm^{-1}, 10 cm^{-1} lower than for Pt/Al_2O_3, the shift being attributed to dilution of the Pt surface by Ge. Similarly, the substitution of a Pt atom in a Pt(111) surface by a Ge atom in a Pt(111)–Ge surface alloy slightly shifted the ν(CO) band to lower wavenumbers (26). Here the shifts, particularly after calc and oxy treatments, were in the opposite sense, but nevertheless agreed with results for chlorided (24) and fluorided (5) Pt–Ge/Al_2O_3. The negligible shift here for catalysts after ox cycles contrasts with the shifts of ca. +10 cm^{-1} after calc or oxy cycles, suggesting that the results were strongly dependent on catalyst pretreatment. Garetto *et al.* (22–24) reported shifts in both directions depending on the catalyst reduction temperature, $\Delta\nu$(CO) being −4 or +12 cm^{-1} after reduction at 573 or 773 K, respectively. The latter result, which resembles the dominant result here for well-dispersed Cl-containing Pt–Ge/Al_2O_3, was attributed to an electronic effect involving electron transfer from Pt to Ge. An XPS study established that Pt in Pt–Ge/Al_2O_3 was more electron-deficient than Pt in Pt/Al_2O_3 (8) in accordance with this conclusion.

The ν(CO) band due to linearly adsorbed CO on arrays of Pt atoms in Pt–Sn/Al_2O_3 catalysts was moved to lower wavenumbers with respect to ν(CO) for CO on Pt/Al_2O_3 when alloy particles of 1 : 1 Pt^0–Sn^0 stoicheiometry were formed during catalyst reduction (13), but moved to higher wavenumbers when the Pt was present as Pt^0 particles on which surface atoms were rendered e-deficient by interaction with SnO_x species spread over the alumina surface. The former may be attributed to the combination of an electronic effect due to e-transfer from Sn^0 to Pt^0 in alloy surfaces, and a geometric effect due to much reduced lateral dipolar coupling interactions between adjacent CO molecules on the alloy surfaces than on particles composed entirely of Pt^0. Borgna *et al.* (24) ascribed a positive $\Delta\nu$(CO) shift, similar to that here, on adding Ge to Pt/Al_2O_3 to the formation of alloyed Pt–Ge particles on which Pt atoms were influenced by Ge acting as an e-acceptor. Dilution of surface Pt sites by Ge would lead to reduced dipolar interactions and a competing downward band shift particularly at high surface coverages (25). Ge on a Pt(111) surface shifted the ν(CO) band downward rather than upward, and therefore any electronic effect of Ge^0 on Pt^0 is also apparently in the wrong sense to be consistent with an enhancement in the electrophilic character (24) of Pt. The XRD work here shows that alloy particles were not formed in the present catalysts, at least in the sense of a regular bulk-phase crystalline structure or a solid solution of Ge in Pt.

The surface character of Pt in Pt–Ge/Al_2O_3 is influenced by reduction temperature (24). Reduction at 573 K gave Pt particles with a chlorided alumina support and with nonreduced GeO_x particles. Raising the reduction temperature from 573 to 773 K gave two germanium phases, GeO_x and metallic germanium, the latter closely interacting with the Pt. Here a reduction temperature of 673 K probably (4–8) led to catalyst in which none or only very little of the germanium was present as Ge^0. This conclusion is consistent with the present CO/Pt results for which the effects of Ge for Cl-free catalysts were similar to those for catalysts reduced at 573 K (24) and for Cl-containing catalysts which actually showed an improved dispersion rather than a significant loss. The positive shift $\Delta\nu$(CO) on adding Ge to Pt/Al_2O_3 particularly after oxy cycles, is therefore primarily attributed to CO on Pt sites rendered e-deficient by electron transfer to a germania-modified alumina surface. The band at 2071 cm^{-1} for adsorbed CO after calc and ox cycles reflects the effect of GeO_x-modification of alumina on the band positions. The higher position of 2081 cm^{-1} after oxy cycles reflects an added effect of chlorine. The latter could be a direct e-withdrawing effect of Cl adatoms on the Pt surface (13, 14). The existence of Pt–Cl species in reduced chlorinated Pt–Ge/Al_2O_3 has been detected by EXAFS (24). The shift in the ν(CO) band position to higher wavenumber (1900 cm^{-1}) for bridged CO on Pt–Ge/Al_2O_3 may similarly be ascribed to e-withdrawing effects of Cl (14). The dominant ν(CO) band positions for Pt/Al_2O_3 of 2060, 2072, and 2072 cm^{-1} after calc, ox, and oxy cycles, respectively, which became 2071, 2071, and 2081 cm^{-1} for Pt–Ge/Al_2O_3 compare with 2071, 2071, and 2080 cm^{-1} for low-loaded Pt–Sn/Al_2O_3 (14), suggesting that Ge and Sn addition had similar effects on Pt site character. The results for Pt–Sn/Al_2O_3 are discussed in detail elsewhere (14) and differ significantly from corresponding results for high-loaded Pt–Sn/Al_2O_3 in which Pt^0–Sn^0 alloy particles were formed after an oxy cycle (13).

Shifts in ν(CO) to higher wavenumber with increasing surface coverage may be due either to enhanced dipolar coupling interactions between adjacent CO molecules or to site heterogeneity leading to adsorption on the lowest coordination or the least electron-deficient Pt sites at the lowest coverages. The shifts were much smaller for Pt–Ge/Al_2O_3 than for Pt/Al_2O_3, primarily because the

addition of Ge caused bigger increases in ν(CO) at low coverages (ca. 2–5% coverage for the lowest CO pressure studied) than at high coverages. Thus, for example, ν(CO) values at low coverage for Pt–Ge/Al_2O_3, irrespective of Ge loading, were 2062, 2063, and 2075 cm^{-1} after calc, ox and oxy cycles, respectively, compared with 2040, 2042, and 2052 cm^{-1} for Pt/Al_2O_3. The corresponding shifts with increasing coverage were therefore ca. 9, 8, and 6 cm^{-1} for Pt–Ge/Al_2O_3 compared with 20, 30, and 20 cm^{-1} for Pt/Al_2O_3. Factors which might be considered in relation to these results are geometric effects due to reductions in Pt ensemble size (25), electronic effects due to electron withdrawal from Pt induced by Ge (8, 22–24), and Pt site heterogeneity (16).

If dipolar coupling interactions between adjacent adsorbed CO molecules increase with increasing coverage, then a reduction of Pt ensemble size caused by decoration of the surface by Ge (6, 25) should reduce the dipole coupling shift in accordance with the present results. However, this cannot alone account for the significant shift to higher wavenumber for CO at low coverages on adding Ge to Pt/Al_2O_3. The alternative premise that dipolar coupling interactions are also important at low coverages because of clustering of adsorbed CO molecules (27) would only be consistent with the results here if clustering at low coverage occurred for Pt–Ge but not for Pt alone, and there appears to be no obvious reason why this should be so. Electron withdrawal from Pt induced by the addition of germanium could account, as at high coverages, for the shift of ν(CO) to higher wavenumbers at low coverages, and the even higher band position after oxy cycles may result from an enhanced e-withdrawing effect in the presence of chlorine. Thus strong e-withdrawing effects of GeO_x and Cl apparently have the dominant influence on Pt site character, but geometric effects due to decoration of the Pt surface by Ge reduce ensemble size (6) and therefore reduce dipolar coupling interactions at high CO coverages of the Pt surface. The influence of germanium on the ν(CO) band positions at low coverage is primarily due to electronic effects, whereas at high coverages the dominance of the electronic effects is partially compensated by reduced dipolar coupling effects compared with those for Pt alone.

A Pt(0.3%)/Al_2O_3 catalyst showed evidence for site heterogeneity which was particularly apparent from the results of coking experiments (16). Low and intermediate coordination Pt atoms constituted the strongest adsorption sites and therefore the ν(CO) band envelopes for low coverages were at lower wavenumbers than for CO on medium sized or large ensembles of highly coordinated Pt atoms. The absence of the low wavenumber bands for Pt–Ge/Al_2O_3 shows that either the low coordination Pt sites were blocked or removed by Ge, or the sites were rendered more e-deficient by the electron-withdrawing effects of GeO_x and also, after oxy cycles, Cl. The low wavenumber bands for Pt alone were replaced by bands at higher wavenumbers for Pt–Ge and did not simply just disappear. Thus low coordination Pt sites were apparently not blocked or removed by Ge, but were subjected to e-withdrawal by the GeO_x-modified alumina surface. Overall, however, the small shifts in the ν(CO) band maximum with coverage for the Pt–Ge/Al_2O_3 catalysts suggests that the majority of the exposed Pt atoms were closely similar to each other in character. The implications of the infrared results are, therefore, that platinum in the present Pt–Ge/Al_2O_3 catalysts was sufficiently well spread over the GeO_x-modified alumina surface for all the Pt atoms to be rendered electron-deficient by interaction with the oxidic surface, but that the size of exposed Pt ensembles was reduced either by surface decoration with germanium or by being broken up into smaller patches by oxidic germanium on the alumina surface. All the germanium except for the small amount decorating the Pt surfaces was in the Ge^{2+} or Ge^{4+} states, and there were no bulk-phase Pt–Ge alloys or solid solutions present.

Catalyst Activities

Activities and TOFs for hydrocarbon reactions over Pt–Ge/Al_2O_3 which had been prereduced at 773 K were reported to be considerably lower than those for Pt/Al_2O_3 (4, 7). However, reduction temperatures less than 623 K gave Pt–Ge catalyst with activities approaching those for Pt alone (7). This contrasting behavior was attributed to reduction of germanium to the Ge^0 state at higher temperatures, leading to catalyst deactivation. Here, catalyst activity was maintained at a fairly high level for Pt–Ge/Al_2O_3 after reduction at 673 K, further suggesting that only a very small proportion of the Ge present had been reduced to Ge^0.

The general enhancement (except for the first oxy cycle after ox cycles) in catalyst activities induced by the presence of chlorine (Fig. 5) is consistent with previous reports (4, 11). However, this was accompanied by bigger proportional increases in the numbers of exposed Pt sites (Fig. 3), therefore resulting in Cl-induced decreases in TOF values. Thus, both Ge addition and Cl addition led to small decreases in TOF values, which may be related to the e-withdrawing effects of GeO_x or Cl decreasing the electron density at exposed Pt sites which were actively involved in catalysis.

Catalyst Selectivities

The effects on catalyst selectivity of adding Ge to Pt/Al_2O_3 contrast with the corresponding effects of Sn (21). For Cl-free catalysts the main difference involved hydrogenolysis which was increased by Sn but decreased by Ge, the balance for Ge being reflected in better selectivities for isomerisation and cyclization. The differences between the effect of Sn and that of Ge were even greater when chlorine was present. Compared with aromatization and cyclization down and hydrogenolysis up and isomerization

slightly up on adding Sn, Ge greatly reduced hydrogenolysis and increased aromatization to a small extent and isomerization and cyclization by greater but about equal amounts. These results were accompanied by higher overall activities for Ge- rather than Sn-containing catalysts even though the Ge loadings (in terms of mol per gram of catalyst) were higher for Ge than for Sn.

The addition of Ge to Pt/Al_2O_3 has previously been found to reduce cyclopentane hydrogenolysis activity (4, 7), particularly after high-temperature reduction had promoted Ge^0 formation. Octane hydrogenolysis selectivities were much lower over Pt–Ge/Al_2O_3 than over Pt/Al_2O_3 (6). Increasing Ge content reduced the TOF for hydrogenolysis of butane (5). The decreases in hydrogenolysis TOF for catalysts in which some Ge^{4+} had been reduced to Ge^{2+} were ascribed to an electron-withdrawing effect on Pt of reduced Ge^{2+} ions (5), an explanation which is consistent with the present infrared results, but contrasts with the possible expectation (28, 29) that e-deficient Pt sites would favor hydrogenolysis.

A decrease in hydrogenolysis selectivity also accompanied increasing Pt particle size in Pt/Al_2O_3 catalysts after repeated ox cycles, the effect of oxychlorination being conversely to reduce particle size and increase hydrogenolysis (21). The results for Pt–Ge/Al_2O_3 after oxy cycles were therefore more akin to those for big rather than small Pt particles. A similar effect has been reported from a study of the hydrogenolysis of 2,2,3,3-tetramethylbutane over Pt–Ge/Al_2O_3 (12). A plausible explanation, consistent with the CO chemisorption and infrared results, would be that extended ensembles of Pt atoms were favored by efficient spreading (as mats rather than small three-dimensional clusters?) of Pt over a GeO_x-modified alumina surface, the surface of the arrays being only partially decorated by Ge. In contrast, for Pt–Sn/Al_2O_3 (21) the extent of spreading of Pt was considerably less than for Pt–Ge/Al_2O_3 and the exposed particle surfaces were largely decorated by Sn leaving only small ensembles of exposed Pt which behaved in a similar way to the surfaces of small Pt^0 particles.

The C_1/C_3 ratios for Cl-containing Pt/Al_2O_3 (21) and Pt–Ge/Al_2O_3 were nearly identical to each other, suggesting that the addition of Ge had negligible effect on the ratio of terminal to central C–C bond fission in the hydrogenolysis reactions. A reduced preference for terminal fission induced by Sn addition to Pt/Al_2O_3 (21) has been ascribed to the blockage by Sn of low coordination Pt sites. The contrasting behavior of Ge and Sn supports the infrared evidence that Ge did not block low-coordination Pt sites.

The decreases in aromatization selectivities with time-on-line for Pt–Ge/Al_2O_3 agree with results for one other catalyst, but contrasts with results for three Pt(0.3%)–Ge(0.3%)/Al_2O_3 catalysts prepared by different methods (6). Also with one exception, the aromatization selectivities for Cl-containing Pt–Ge/Al_2O_3 were less than those for Pt/Al_2O_3. Here, the addition of Ge caused a decrease in selectivity for Cl-free catalysts, but an increase when Cl was present further emphasizing the influence of catalyst composition and preparation procedure (6) on catalytic behavior. The electronic character of Pt sites (28, 30), the local stereochemistry of the sites (31), and the size of Pt ensembles (32) all influence selectivities. Here, the combination of Ge and Cl favored aromatization selectivity possibly because of combined effects of a more e-deficient site character, which has been linked to aromatization enhancement over Pt–Sn/Al_2O_3 catalysts (28), and of the presence of step and kink sites which were not blocked by Ge and are particularly active for aromatization reactions (31). Oxy cycle treatment of Pt–Sn/Al_2O_3 catalyst reduced (14) or inhibited (13) aromatization of heptane because of geometric effects associated with either considerable decoration of the Pt surfaces with Sn (14) or alloy formation (13). The enhancement in aromatization selectivities here for Pt–Ge/Al_2O_3 compared to Pt/Al_2O_3 after oxy cycles could be taken as further suggesting that Pt–Ge alloy was not formed and that the extent of decoration of Pt by Ge was far less than that by Sn.

There are conflicting reports as to whether Ge addition to Pt/Al_2O_3 decreases (6, 33) or, as here for both Cl-free and Cl-containing catalysts, increases (5, 11) isomerization selectivity. The isomerization selectivities must be accountable in terms of significant contributions from bond-shift mechanisms because the high 2MH/3MH and 3EP/3MH ratios (up to 4.7 for 3EP/3MH over Pt/Al_2O_3) cannot be rationalized solely in terms of nonselective cyclic mechanisms. The alumina surface coated with germania is both Lewis and Brønsted acidic (34) but has been reported to be catalytically inactive up to 723 K with or without chlorine present (5, 11) or slightly active at 783 K (6) in hydrocarbon reforming reactions. Therefore, in the present catalysts at 623 K it is probable that the dominant isomerization reactions involved metallic Pt, either on its own or as part of a bifunctional catalyst acting in conjunction with the oxide support.

The addition of Ge had contrasting effects on the selectivities to 2MH in the sense that for Cl-free catalyst 2MH became less significant relative to the other isomers, whereas for Cl-containing catalysts 2MH was enhanced. This was in parallel to a decrease in toluene selectivity for Cl-free catalysts and an enhancement in toluene for Cl-containing catalysts. On the basis of a cyclic mechanism for 2MH formation, an adsorbed methylcyclohexane intermediate would be required (35) and this would also be a precursor of toluene, thus suggesting perhaps that a cyclic mechanism was at least partially responsible for the effects of chlorine on isomerization behavior. However, the majority of the 2MH, and also 3MH and 3EP, resulting from catalysis must have been formed by bond-shift mechanisms (35). In apparent support of this conclusion was the negligible effect of Ge on the cyclization DMCP/ECP ratios for

Cl-containing catalysts, in contrast to the significant changes in isomerization product ratios.

Oxychlorination of Pt–Sn/Al_2O_3 catalysts (13, 21) considerably enhanced DMCP formation at the expense of ECP and this was ascribed to the blocking of low-coordination Pt sites by Sn or to Pt–Sn alloy formation which had the biggest effect and completely eliminated ECP as a product (13). The negligible change in DMCP/ECP for Cl-containing Pt–Ge/Al_2O_3 compared with Pt/Al_2O_3 further confirms the absence of Pt–Ge alloy formation and supports the conclusions that the Pt surface was only slightly decorated by Ge and blocking of low coordination sites did not occur. The similar DMCP/ECP values for Cl-free and Cl-containing Pt–Ge/Al_2O_3 are also consistent with these conclusions, and contrast with the large Cl-induced changes in selectivity ratios for isomerization products which probably resulted from dominant effects of oxychlorination on bond-shift mechanisms of catalysis.

The reduction in aromatization selectivity and the reduced 2MH selectivity with respect to 3MH and 3EP during coking were similar for Pt–Ge/Al_2O_3, Pt/Al_2O_3 (21), and Pt–Sn/Al_2O_3 (21). The effect of Ge on Pt/Al_2O_3 in lessening the deactivation by coking has been reported by de Miguel *et al.* (4) and Huang *et al.* (6), although the effect was not as great as the enhanced catalyst stability induced by Sn (21). Less coke is formed on Pt–Ge than on Pt alone (6, 36).

CONCLUSIONS

For Pt(0.3%)–Ge/Al_2O_3 catalysts containing 0.15 or 0.45% Ge after reduction at 473K:

(a) Ge predominantly existed as Ge^{4+} and Ge^{2+} ions in a GeO_x-modified alumina surface; Ge did not block low-coordination Pt sites but may have partially decorated arrays of high-coordination Pt atoms;

(b) no bulk-phase Pt^0–Ge^0 alloys or solid solutions were formed; clusters of Pt^0 atoms were influenced by the e-withdrawing effects of GeO_x on alumina and Cl-adatoms on Pt;

(c) catalytic activity was hardly compromised by the addition of Ge to Pt/Al_2O_3 although Ge improved resistance to activity loss with increasing time-on-line;

(d) the mutual addition of Ge and Cl to Pt/Al_2O_3 favored aromatization, isomerization, and cyclization reactions at the expense of hydrogenolysis;

(e) oxychlorination led to the generation of oxychloro-Pt complexes which spread over the support surface and, as for Pt/Al_2O_3, favored good Pt dispersion after subsequent reduction.

ACKNOWLEDGMENTS

We thank the Consejo Nacional de Investigaciones Cientificas y Tecnologicas, Venezuela, and the University of Zulia, Venezuela, for a studentship (G.J.A.) and The Royal Society (London) for a University Research Fellowship (J.A.A.).

REFERENCES

1. Anderson, J. A., Mordente, M. G. V., and Rochester, C. H., *J. Chem. Soc. Faraday Trans.* **85**, 2983 (1989).
2. Anderson, J. A., Mordente, M. G. V., and Rochester, C. H., *J. Chem. Soc. Faraday Trans. 1* **85**, 2991 (1989).
3. Mordente, M. G. V., and Rochester, C. H., *J. Chem. Soc. Faraday Trans. I* **85**, 3495 (1989).
4. De Miguel, S. R., Scelza, O. A., and Castro, A. A., *Appl. Catal.* **44**, 23 (1988).
5. Goldwasser, G., Arenas, B., Bolivar, C., Castro, G., Rodriguez, A., Fleitas, A., and Giron, J., *J. Catal.* **100**, 75 (1986).
6. Huang, Z., Fryer, J. R., Park, C., Stirling, D., and Webb, G., *J. Catal.* **175**, 226 (1998).
7. De Miguel, S. R., Correa, J. A., Baronetti, G. T., Castro, A. A., and Scelza, O. A., *Appl. Catal.* **60**, 47 (1990).
8. Bouwman, R., and Biloen, P., *J. Catal.* **48**, 209 (1977).
9. Hansen, M., and Anderko, K., "Constitution of Binary Alloys." McGraw-Hill, New York, 1958.
10. Castanet, R., *J. Chem. Thermodyn.* **14**, 639 (1982).
11. Aboul-Gheit, A. K., Menoufy, M. F., and Ebeid, F., *Appl. Catal.* **4**, 181 (1982).
12. Coq, B., Chaqroune, A., Figueras, F., and Nciri, B., *Appl. Catal.* **82**, 231 (1992).
13. Arteaga, G. J., Anderson, J. A., Becker, S. M., and Rochester, C. H., *J. Mol. Catal. A*, in press.
14. Arteaga, G. J., Anderson, J. A., and Rochester, C. H., *J. Catal.* **184**, 268 (1999).
15. De la Cruz, C., and Sheppard, N., *Spectrochim. Acta A* **50**, 271 (1994).
16. Arteaga, G. J., Anderson, J. A., and Rochester, C. H., *Catal. Lett.* **58**, 189 (1999).
17. Barshad, Y., Zhou, X., and Gulari, E., *J. Catal.* **94**, 128 (1984).
18. Parkyns, N., *J. Chem. Soc. A*, 1910 (1967).
19. Parkyns, N., *J. Chem. Soc. A*, 410 (1969).
20. Irving, R. J., and Magnussen, E. A., *J. Chem. Soc.* 1860 (1956) and 2283 (1958).
21. Arteaga, G. J., Anderson, J. A., and Rochester, C. H., *J. Catal.* **182**, 219 (1999).
22. Garetto, T. F., Borgna, A., and Apesteguía, C. R., *Stud. Surf. Sci. Catal.* **101**, 1155 (1996).
23. Garetto, T. F., Borgna, A., and Apesteguía, C. R., *Stud. Surf. Sci Catal.* **88**, 369 (1994).
24. Borgna, A., Garetto, T. F., Apesteguía, C. R., and Moraweck, B., *Appl. Catal. A* **182**, 189 (1999).
25. De Ménorval, L.-C., Chaqroune, A., Coq, B., and Figueras, F., *J. Chem. Soc. Faraday Trans. 1* **93**, 3715 (1997).
26. Fukutani, K., Magkoev, T. T., Murata, Y., Matsumoto, M., Kawauchi, T., Magome, T., Tezuda, Y., and Shin, S., *J. Electron Spectrosc. Relat. Phenom.* **88**, 597 (1998).
27. Primet, M., *J. Catal.* **88**, (1984) 273.
28. Burch, R., and Garla, R. L. C., *J. Catal.* **71**, 360 (1981).
29. Zhuang, Y., and Frennet, A., *Appl. Catal. A* **134**, 37 (1996).
30. Coq, B., and Figueras, F., *J. Catal.* **85**, 197 (1984).
31. Davis, S. M., Zaera, F., and Somorjai, G. A., *J. Catal.* **77**, 439 (1982).
32. Paál, Z., Gyóry, A., Uszkurat, I., Olivier, S., Guérin, M., and Kappenstein, C., *J. Catal.* **168**, 164 (1997).
33. Al-Kady, G. M., Al-Ahmadi, A. A., Menoufy, M. F., and Aboul-Enin, H., *Indian J. Technol.* **31**, 846 (1993).
34. Katada, N., Niwa, M., and Sano, M., *Catal. Lett.* **32**, 131 (1995).
35. Somorjai, G. A., "Chemistry in Two Dimensions—Surfaces." Cornell Univ. Press, Ithaca, NY, 1981.
36. Beltramini, J. N., and Datta, R., *React. Kinet. Catal. Lett.* **44**, 353 (1991).